D2.2 | First Complete Detector
Authors: Maria Spies, Elia Strambini
Delivery date: 15.12.2021
Version: 1.0

This project has received funding from the European Union's Horizon 2020 research and innovation programme under grant agreement No 800923.

Project Acronym:	SUPERTED
Project Full Title:	Thermoelectric detector based on superconductor-ferromagnet heterostructures
Call:	H2020-FETOPEN-2016-2017
Topic:	FETOPEN-01-2016-2017
Type of Action:	RIA
Grant Number:	800923
Project URL:	https://superted-project.eu/

Editor:	Maria Spies, CNR Pisa; Elia Strambini, CNR Pisa
Deliverable nature:	Report (R)
Dissemination level:	Public (PU)
Contractual Delivery Date:	31.10.2021
Actual Delivery Date:	15.12.2021
Number of pages:	11
Keywords:	Superconducting thermoelectric detector, ferromagnetic insulator- superconductor heterostructures, tunneling spectroscopy, spin-splitting
Author(s):	Maria Spies, CNR Pisa; Elia Strambini, CNR Pisa Zhuoran Geng, University of Jyväskylä, JYU Tatu Korkiamäki, University of Jyväskylä, JYU Ilari Maasilta, University of Jyväskylä, JYU
Contributor(s):	Sanna Rauhamäki, University of Jyväskylä, JYU Tero Heikkilä, University of Jyväskylä, JYU
External contributor(s):	

Abstract

The deliverable 2.2 'First Complete Detector' of Work Package 2 gives an overview of the work carried out in the project during the period from February to October 2021 relating to the elaboration and processing of the final detector for THz and X-ray made of ferromagnetic insulator (FI) and superconductor (S) bilayers. Through cleanroom processing a successful recipe has been elaborated to process the as-grown samples provided by both CSIC and MIT.

This project has received funding from the European Union's Horizon 2020 research and innovation programme under grant agreement No 800923.

1 Fabrication process design for the detector of THz radiation

After the successful demonstration of the effects of rectification and, to a lesser extent, the thermoelectric effect in the previous part of the project (deliverable D2.3), we proceeded to build the first detector. For that, an additional post-processing step is necessary. In the following, the elaboration of the first THz detector is outlined. The progress on the x-ray detection is reported in the next section. Here we outline the design and optimization of the THz antenna obtained via additional cleanroom processing on the best samples characterized during SUPERTED. Both have been carried out for the two sample structures we have been working with from the beginning, which originate from the two different sample suppliers within the project:

- samples from CSIC: Si substrate/ SiO2/ EuS/ Al/ AlOx barrier/ Co/ CaF protective layer
- samples from MIT: fused silica substrate/ Cu/ EuS barrier/ Al/ Al2O3 protective layer

1.1 Antenna design

The original proposed design was the one shown in Fig.1. The basic idea is to reshape the superconducting lead to form an antenna suitable for the absorption of THz radiation.

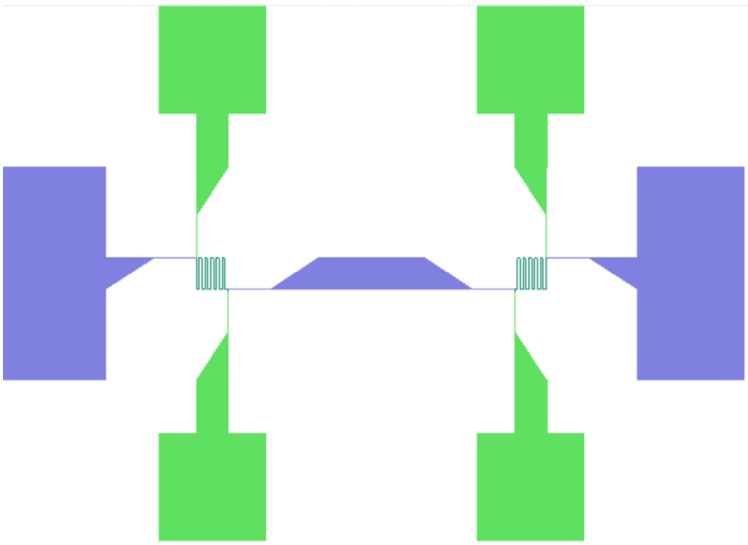

Figure 1: Sample sketch of the processed superconductor-ferromagnetic insulator bilayer tunnel junctions used for THz detection.

The typical cross-bar shape of the samples is visible and the different material components are drawn in different colors (green and blue for Co and Al (CSIC) or Al and Cu (MIT), respectively). This design has been modified on several points. (i) Only the Al is being etched rather than also the Cu or Co strip. This is where the THz radiation will be absorbed. The other component can remain passive in this step. (ii) The junction is kept in its original shape instead of being etched. This will minimize possible degradation of the tunnel barrier. (iii) Due to the lack of sharpness of the corners of the strips of the as-grown samples the thin line connecting to the outer contact pads is placed in the middle of the original strip rather than on the outside.

Therefore, for the optimal absorption of THz radiation the following design has been elaborated. The Al strip is etched into the relevant shape. The Al lines have a thickness of 5 μm.

This project has received funding from the European Union's Horizon 2020 research and innovation programme under grant agreement No 800923.

There are five parallel lines with a spacing of 25 μm and a length of 770 μm. The junction itself is not etched.

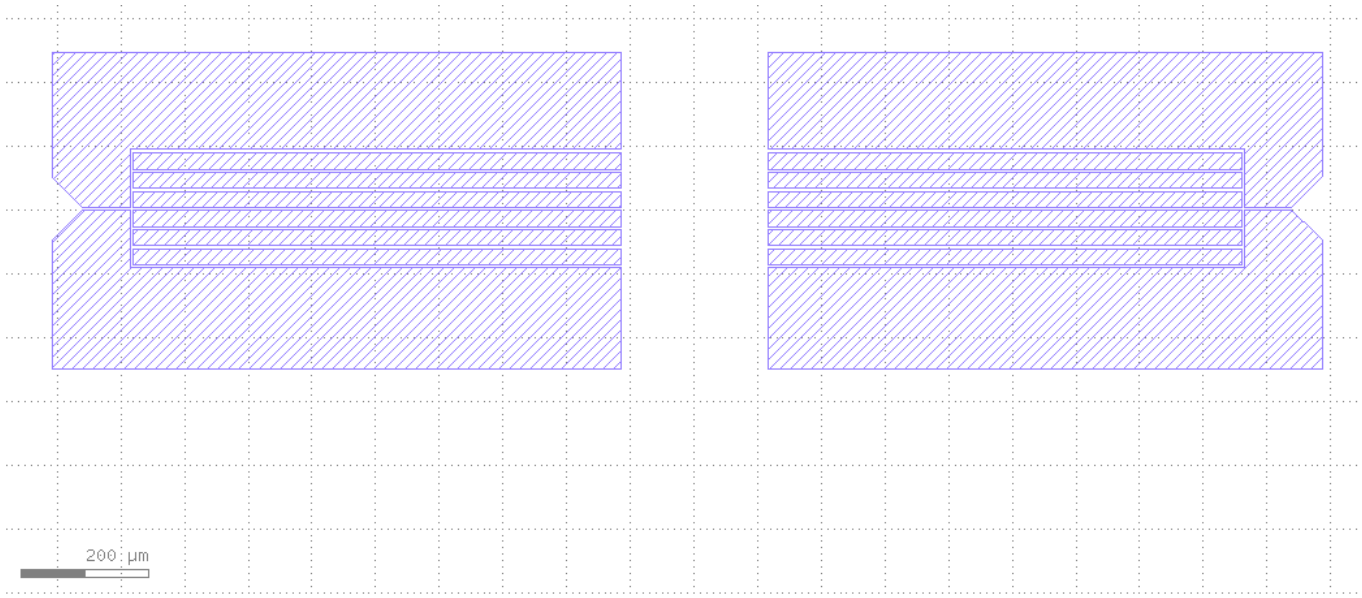

Figure 2: Final optical lithography mask used to process the as-grown samples into the final detector. The tunnel junction is in the middle between the exposed areas.

This project has received funding from the European Union's Horizon 2020 research and innovation programme under grant agreement No 800923.

1.2 Etching tests and recipe development

The original recipe was adapted from lift-off techniques and it was successfully used for samples from both CSIC and MIT.

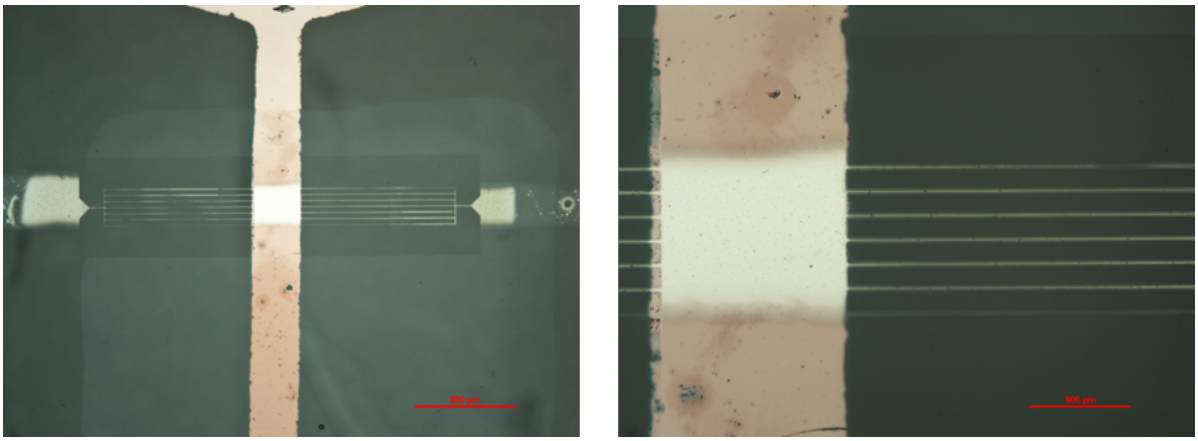

Figure 3: Optical microscope images of etching tests on the MIT sample "10223 Cu bottom G 40A EuS part 2" made with recipe 1. The vertical strip is the unetched Cu, the horizontal Al is etched. The light, rectangular contrast on the left image is the protective layer which has not been etched. The red scale bar is 500 μm.

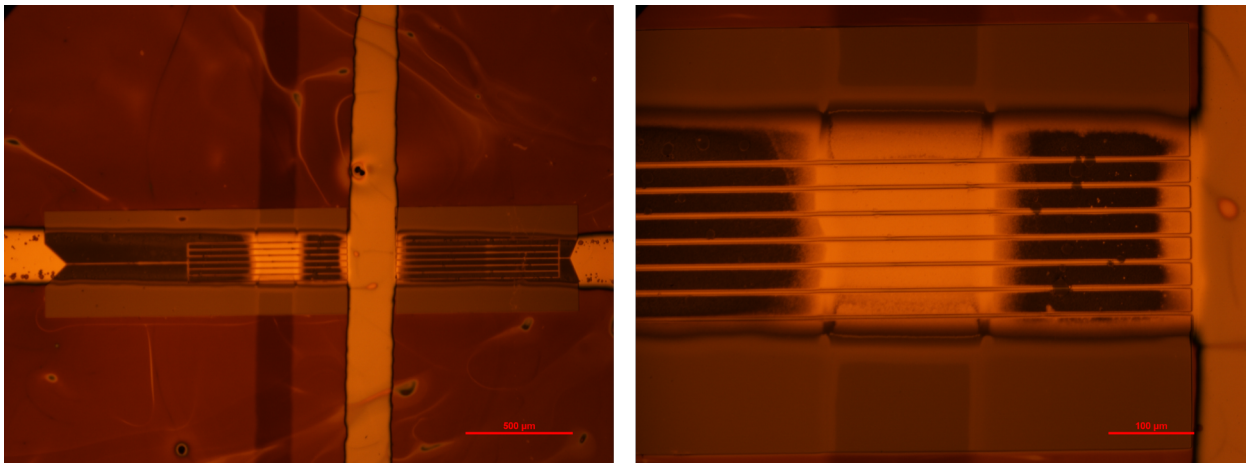

Figure 4: Optical microscope images of etching tests on the CSIC sample "210702-S2" made with recipe 1 (image taken with an orange filter while the resist is still on the sample). The vertical strip is the unetched Co (the shadow-like vertical strip as well, due to a growth problem), the horizontal Al is etched. The scale bar is 500 μm.

Recipe 1:

- 3 min acetone ultrasound, 3 min IPA ultrasound for cleaning
- Resist 1: PMMA AR-P 679.02: 5 sec 500 rpm, 1 min 6000 rpm, bake at 170°C for 90 sec
- Resist 2: LOR3A: 5 sec 500 rpm, 1 min 5000 rpm bake at 190°C for 3 min
- Resist 3: S1805 on 5 sec 500 rpm, 1 min 5000 rpm bake at 110°C for 1 min
- Development: 45 sec MF 319 which develops the exposed S1805 (and LOR3A) + DI rinse
- O2 plasma for 8 min at 30 W

This project has received funding from the European Union's Horizon 2020 research and innovation programme under grant agreement No 800923.

- wet etching of Al: MF 319: 50 sec
- all is lifted with 15 min Acetone bath at 50°C

The PMMA layer protects the Al from the LOR3A resist which can only be taken off with an Al etchant (MF319). The O2 plasma is used to open the PMMA where the S1805 has been exposed. The Al2O3 layer (MIT samples) and the CaF (CSIC samples) can be etched with MF319. It therefore occurs during the etching of the Al layer (same etchant).

The recipe was adapted in the following because the LOR3A is a resist which dissolves only in the Al etchant MF319. This continually endangers the samples while working with them. The LOR3A layer has been removed from the recipe.

Recipe 2:

- 3 min acetone ultrasound, 3 min IPA ultrasound for cleaning
- Resist 1: PMMA AR-P 679.02: 5 sec 500 rpm, 1 min 6000 rpm, bake at 170°C for 90 sec
- Resist 2: S1805 on 5 sec 500 rpm, 1 min 5000 rpm bake at 110°C for 1 min
- Development: 45 sec MF 319 which develops the exposed S1805 (and LOR3A) + DI rinse
- O2 plasma for 8 min at 30 W
- wet etching of Al: MF 319: 50 sec
- all is lifted with 15 min Acetone bath at 50°C

This project has received funding from the European Union's Horizon 2020 research and innovation programme under grant agreement No 800923.

2 Fabrication process design for SuperTED as micro-calorimeter

Two core structures are important to a micro-calorimeter for keV X-ray sensing. One structure must stop and absorb the incident photon, converting its energy into heat or other measurable excitations, whereas the other structure must transduce the heat or excitations into an electrical signal that can be measured. The latter structure in the SuperTED project is a sensor device made of EuS/Al/AlOx/Co tunnel junctions fabricated at CSIC, whereas the former structure, called the absorber, is fabricated in JYU after the tunnel junction device is made.

2.1 Detector design and fabrication processes

The absorber structure requires a clean contact to the sensing electrode, and the absorbed photon energy is required to be temporarily confined in a finite volume body for calorimetry. Therefore, several consecutive additional fabrication steps are required after the first processing round at CSIC that produces the tunnel junction chip. The proposed detector design is shown in Fig. 5 (a).

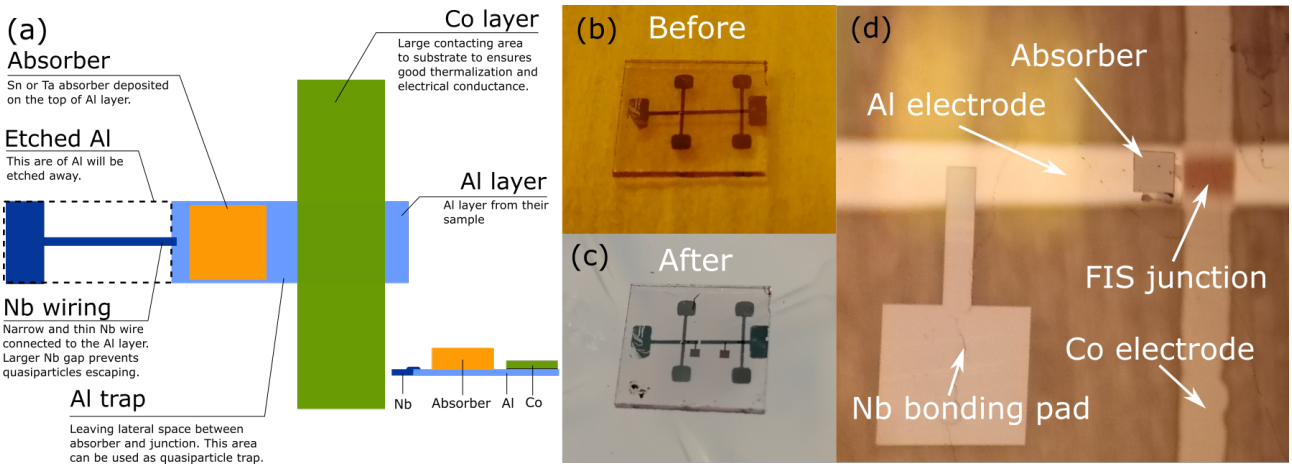

Figure 5: (a) Schematic of the proposed micro-calorimeter design based on ferromagnetic-insulator-superconductor (FIS) heterostructure. (b) and (c) show the detector chip before and after fabrication processes. (d) Zoom-in image on one detector.

The sample used for the first demonstration of the absorber processing consists of a fused silica substrate on top of which a EuS/Al/AlOx barrier/Co/CaF multilayer structure, and the tunnel junctions were defined in a hall-bar shape as shown in Fig. 5 (b). Four consecutive fabrication steps were designed and optimized, and the protocol was carried out and validated on the received sample. The result is shown in Fig. 5 (c) and (d). In the following we elaborate the fabrication protocols.

The first step is to separate the two junctions and to define the sensitive volume of the Al electrode by defining a certain length in the middle of the Al strip by etching away portions of the Al strip. The remaining Al electrode that connects the junction is designed to be 200 μm wide and 170 μm long. It should be noted here that in the fabrication validation sample demonstrated in this report, we did not apply the same design dimensions due to the charging effect of fused silica substrate during electron-beam lithography. The next batch of samples, provided to us already, use substrates with 525 nm SiN on the top of 525 μm silicon to mitigate the charging problems. A standard Al wet etching process was used with a resist (PMMA) mask defined by electron-beam (e-beam) lithography. We have also tested and finalized a

This project has received funding from the European Union's Horizon 2020 research and innovation programme under grant agreement No 800923.

plasma dry etch (RIE) recipe for removing the CaF (7 nm) protective layer on the Al electrode. The workflow of this process is shown in Fig. 6

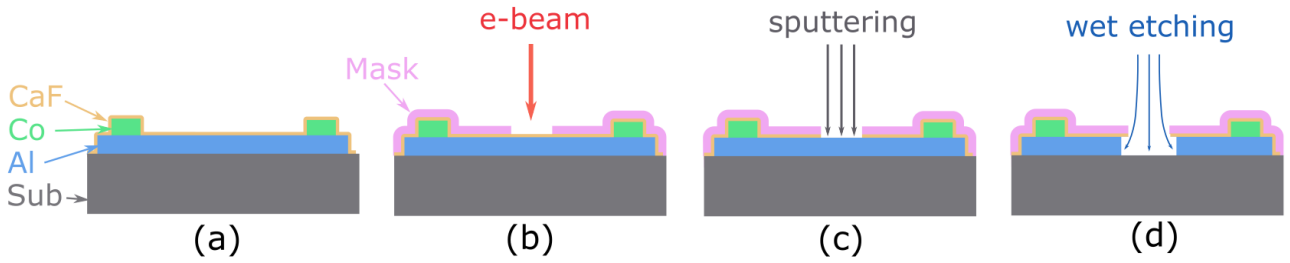

Figure 6: Defining the Al electrode: (a) The sample prepared in CSIC has symmetric junctions on each end of the Al strip that was covered with a thin CaF protective layer. (b) Electron beam lithography is used to define the etching area on the resist mask. (c) CaF layer is dry etched at the defined area. (d) Chemical etching is used to remove Al from the metal strip.

The contacts between the Al electrode and the absorber as well as those to Nb leads are fabricated in the second step. E-beam and RIE were carried out first to define the mask and remove the CaF layer. Native aluminum oxide (AlOx) over the Al electrodes was removed by an Ar sputtering process prior to a deposition of a thin Au (4 nm) without breaking the vacuum. This process is intended to provide a good electrical contact and prevents oxidization of the Al layer in the process steps that follow. The workflow is shown in Fig. 7

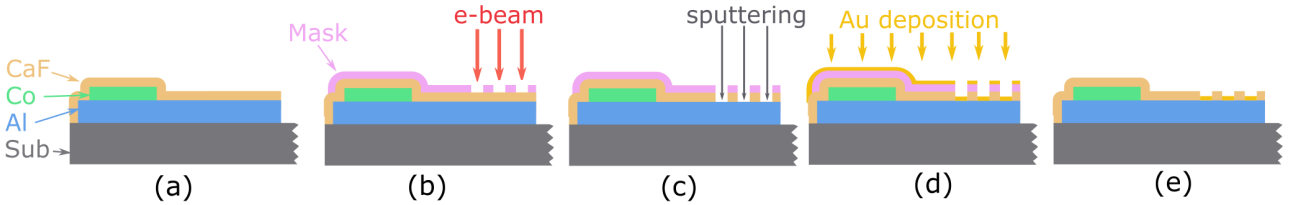

Figure 7: Defining contacts for the absorber and the Nb leads. (a) Single junction prepared by the previous process step. (b) E-beam is used to define the areas of the contacts on a PMMA resist mask. (c) CaF and native AlOx is etched and sputtered. (d) Au thin film is deposited at the contact areas without breaking vacuum. (e) Resist is lifted-off after deposition.

The absorber (150×150 μm^2 Sn) is deposited in the third step (see Fig. 8), and finally, in the fourth step, the Nb leads and bonding pads are deposited (see Fig. 9). Both processes include e-beam lithography, followed by metal deposition and lift-off processes.

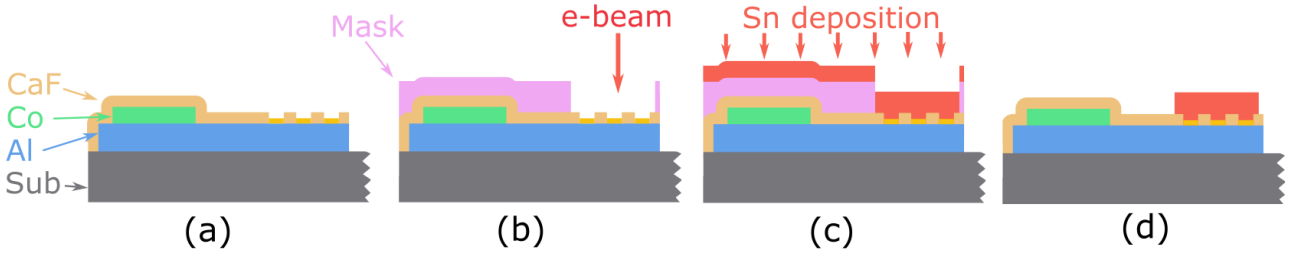

Figure 8: Absorber deposition process. (a) Single junction prepared by the previous process step. (b) E-beam is used to define the areas of the absorber on a PMMA resist mask. (d) Absorber (Sn) is deposited, forming a good galvanic contact with the Al electrode through the Au interlayer. (e) Resist is lifted-off after deposition.

The detailed fabrication recipes of the above protocol are listed in Section 2.3.

This project has received funding from the European Union's Horizon 2020 research and innovation programme under grant agreement No 800923.

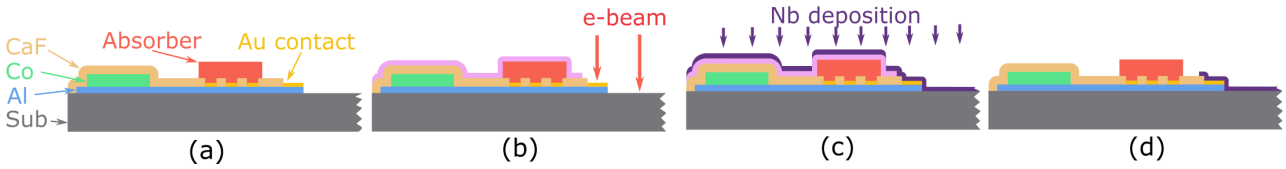

Figure 9: Nb wiring deposition process. (a) Single junction prepared from previous process step. (b) E-beam is used to define the areas of the Nb leads and bonding pad on a PMMA resist mask. (d) Nb is deposited. (e) Resist is lifted-off after deposition.

2.2 Absorber material test

In the presented micro-calorimeter design, the superconducting absorber will be deposited on top of the Al electrode, capable of stopping keV energy range X-rays. A good absorber requires a high X-ray stopping power, a larger energy gap than the Al electrode underneath to allow for the generated quasiparticles to diffuse into Al, and a high diffusion rate so that the pulses are not slowed down. We have tested the deposition of Sn (Z=50, bulk Tc=3.7K), Ta (Z=73, bulk Tc=4.4K), and Nb (Z=41, bulk Tc=9.7K) as options for the absorber material, and characterized their resistivity at cryogenic temperatures. Different evaporation techniques have been experimented for the film deposition. The film quality in our measurement was characterized by the residual resistivity at the critical temperature ($R(T_c)$) and the residual-resistivity-ratio RRR=$R(273K)/R(T_c)$. The material, its deposition technique, the calculated X-ray absorption probability for a 6 keV X-ray photon, the measured resistivity and RRR, and the calculated electron diffusion constant at T_c based on the measured resistivity, are listed in Table 1.

Absorber		X-ray absorption[1] with different absorber thickness			Measured residual resistivity $\rho(T)$		
Material	Deposition technique	0.3 μm	1 μm	5 μm	$\rho(T_c)$ ($\mu\Omega cm$)	RRR	Est. $D_N(T_c)$ (cm^2/s)
Sn	Thermal, 0.2 nm/s	12%	33%	87%	2	21	107
	Thermal, 2 nm/s				1.3	40	164
Ta	E-beam	17%	45%	95%	1250	<1	0.04
	Pulsed laser				200	<1	0.23
	E-beam, Ti seed				850	<1	0.05
	E-beam, Nb seed				440	<1	0.1
Nb	E-beam	8%	25%	76%	77.5	1.3	0.45
	E-beam, Ti seed				75	1.3	0.46

Table 1: Measurement results and estimated X-ray absorption probabilities of different absorber materials tested at JYU with different deposition techniques.

We see from Table 1 that an absorber made of Ta has the best stopping power for 5.9 keV X-rays. However, it is very hard to produce a high quality thin film of Ta with the deposition techniques at our disposal in JYU. Thermally evaporated Sn, with the higher 2 nm/s deposition rate, on the other hand, presents a good compromise with a large stopping power, good film quality and high diffusion rate. The estimated quasiparticle diffusion speed for Sn at 100 mK is $D_{qp} \approx 16$ cm^2/s based on the measurement results, and the observed T_c close to the bulk value. We conclude that such a Sn film with a thickness between 0.3-5 μm will be our choice for the superconducting absorber for the SUPERTED micro-calorimeter.

[1]Absorption for 5.9 keV X-ray, calculated based on Henke B. L., *At. Data Nucl. Data Tables* **54**, 181 (1993).

This project has received funding from the European Union's Horizon 2020 research and innovation programme under grant agreement No 800923.

2.3 Fabrication recipes

1. Defining Al electrode
   (a) Mask layer: PMMA 950, 700 nm, bake at 160 $°C$
   (b) Patterning: 20 kV, 120 μm aperture, 215 $\mu C/cm^2$ area dose
   (c) Development: 40 sec in IPA:MIBK, 1 min IPA rinse
   (d) Dry etching: 2% O_2, 15% SF_6 with 75 W RF power and 50 $mTorr$ pressure, 1 min
   (e) Al wet etching: 30 sec in NaOH
   (f) Mask lift-off: 50 $°C$ in Acetone
2. Defining contacts for absorber and Nb leads
   (a) Mask layer: PMMA 950, 700 nm, bake at 160 $°C$
   (b) Patterning: 20 kV, 120 μm aperture, 215 $\mu C/cm^2$ area dose
   (c) Development: 40 sec in IPA:MIBK, 1 min IPA rinse
   (d) Dry etching: 2% O_2, 15% SF_6 with 75 W RF power and 50 $mTorr$ pressure, 1 min
   (e) Sputtering: 5×10^{-4} $mBar$ Ar, 0.2 A magnetron power, 1 keV extraction voltage, 1 keV beam voltage, 10000 particle counts
   (f) Metal deposition: 4 nm Au, 0.1 nm/s
   (g) Mask lift-off: 50 $°C$ in Acetone
3. Sn absorber deposition
   (a) Mask layer 1: PMMA 950, 700 nm, bake at 160 $°C$
   (b) Mask layer 2: Evaporated Al, 5 nm
   (c) Mask layer 3: PMMA 950, 700 nm, bake at 160 $°C$
   (d) Patterning: 20 kV, 120 μm aperture, 250 $\mu C/cm^2$ area dose
   (e) Development 1: 40 sec in IPA:MIBK, 1 min IPA rinse
   (f) Development 2: 20 sec in NaOH, 1 min DI water rinse
   (g) Development 3: 40 sec in IPA:MIBK, 1 min IPA rinse
   (h) Plasma clean: 100% O_2 with 100 W RF power and 50 $mTorr$ pressure, 20 sec
   (i) Metal deposition: 300 nm Sn with 2 nm/s at 60% power
   (j) Mask lift-off: 50 $°C$ in Acetone
4. Nb wiring deposition
   (a) Mask layer: PMMA 950, 700 nm, bake at 160 $°C$
   (b) Patterning: 20 kV, 120 μm aperture, 215 $\mu C/cm^2$ area dose
   (c) Development: 40 sec in IPA:MIBK, 1 min IPA rinse
   (d) Plasma clean: 100% O_2 with 100 W RF power and 50 $mTorr$ pressure, 20 sec
   (e) Metal deposition: 5 nm Ti seeding layer followed by 20 nm Nb layer
   (f) Mask lift-off: 50 $°C$ in Acetone

This project has received funding from the European Union's Horizon 2020 research and innovation programme under grant agreement No 800923.

3 Outlook

We have achieved a successful development of the fabrication protocol both for the antenna and the absorber on the thermoelectric junction for the implementation of the complete THz and X-ray detectors, respectively. Fabrication is compatible both with CSIC and MIT samples and from preliminary measurements does not show any decrease in the quality of the tunnel junction due to post-processing.

Higher subgap conductance observed in the CSIC samples was a subject of study and optimization. The initial guess was that the subgap conductance originated from defects in the oxide barrier and was checked in a series of experiments. We observed that an additional aluminum layer separating the barrier and the topmost cobalt electrode partially decreases but does not fully eliminate the subgap conductance, but deteriorates at the same time the asymmetry of the spin-dependent tunneling. On the other hand, decreasing of the exchange coupling strength was found to have a stronger effect on the decreasing of the subgap conductivity. These findings allowed us to conclude that the optimization of the devices requires improvement of the interface between the EuS and the bottom aluminum electrode. Next step of the optimization will involve the growing of the EuS and Al layers in a cooled stage (120K) to improve the flatness of the interfaces and decrease the subgap conductance of the tunnel junctions.

The detector is now ready for the electrical DC pre-characterization confirming the quality of the tunnel barrier after etching. Thereafter, the final AC measurements with the THz detector will be carried out by the SUPERTED collaborator, Alessandro Monfardini, in Grenoble according to the road map of the project. The X-ray detector will be tested with an X-ray source in the University of Jyväskylä. Both of these measurements will be carried out during the beginning of the year 2022.

This project has received funding from the European Union's Horizon 2020 research and innovation programme under grant agreement No 800923.